Biogeosciences Discuss., https://doi.org/10.5194/bg-2019-59
Manuscript under review for journal Biogeosciences
Discussion started: 13 March 2019

Biogeosciences Discussions Open Access EGU

Transparent exopolymer particle binding of organic and inorganic particles in the Red Sea: Implications for downward transport of biogenic materials

Abdullah H. A. Dehwah[1,6], Donald M. Anderson[2], Sheng Li[1,4], Francis L. Mallon[3], Zenon Batang[3], Abdullah H. Alshahri[1], Michael Hegy[4], Thomas M. Missimer[5]

[1] King Abdullah University of Science and Technology (KAUST), Water Desalination and Reuse Center (WDRC), Biological and Environmental Science and Engineering (BESE), Thuwal 23955-6900, Saudi Arabia

[2]Woods Hole Oceanographic Institution, Biology Department, Woods Hole, MA 02543, USA

[3]Coastal and Marine Resources Core Laboratory, King Abdullah University of Science and Technology (KAUST), Thuwal, Saudi Arabia

[4]Guangzhou Institute of Advanced Technology, CAS, Haibin Road #1121, Nansha district, Guangzhou 511458, China

[5]U. A. Whitaker College of Engineering, Emergent Technologies Institute, Florida Gulf Coast University, 16301 Innovation Lane, Fort Myers, Florida 33965-6565

[6]Desalination Technologies Research Institute (DTRI), Saline Water Conversion Corporation (SWCC), P.O. Box 8328, Al-Jubail 31951, Saudi Arabia

Biogeosciences Discuss., https://doi.org/10.5194/bg-2019-59
Manuscript under review for journal Biogeosciences
Discussion started: 13 March 2019

Abstract: Binding of particulate and dissolved organic matter in the water column by marine gels allows sinking and cycling of organic matter into deeper water of the Red Sea and other marine water bodies. A series of four offshore profiles were made at which concentrations of bacteria, algae, particulate transparent exopolymer particles (p-TEP), colloidal transparent exopolymer particles (c-TEP), and the fractions of natural organic matter (NOM), including biopolymers, humic substances, low molecular weight neutrals, and low molecular weight acids were measured to depths ranging from 90 to 300 m. It was found that a statistically-significant relationship occurs between the concentrations of p-TEP and bacteria while a minimal, non-significant relationship between p-TEP and algae occurs. This likely reflects the low abundance of larger algal species in the study region. Variation in the biopolymer fraction of NOM in relationship to TEP and bacteria suggests that extracellular discharges of polysaccharides and proteins from the bacteria and algae are occurring without immediate abiotic assembly into p-TEP. In the water column below the photic zone, TOC, bacteria, and biopolymers show a generally common rate of reduction in concentration, but p-TEP decreases at a diminished rate, showing that it persists in moving organic carbon deeper into the water column despite consumption by bacteria.

---

1 Introduction

Biogeosciences Discuss., https://doi.org/10.5194/bg-2019-59
Manuscript under review for journal Biogeosciences
Discussion started: 13 March 2019

Mechanisms that control the biogeochemical cycles influenced by microorganisms in the world ‘s oceans are complex and poorly understood (Azam and Malfatti, 2007). The relationships between microalgal and bacterial abundance, total organic carbon (TOC), fractions of natural organic matter (NOM), polysaccharides, and transparent exopolymer particles (TEP) in seawater with depth play important roles in the transport and cycling of nutrients and sediments (Alldredge and Crocker, 1995; Passow, 2002; Azam and Malfatti, 2007). In particular, the binding of suspended sediments and particulate organic matter by TEP and other acidic polysaccharides, in addition to general aggradation, tends to increase particle size and weight, thus increasing settling rates in the water column (Passow et al., 2001; Wurl et al., 2011). It has been demonstrated that gel-type particles link particulate and dissolved organic matter in the ocean (Verdugo et al., 2004). The sinking of biogenic particles drives elemental cycling, which in turn controls primary and secondary productivity through the water column (Wurl et al., 2011). Particulate organic material is commonly occupied or influenced by bacteria which can reduce the biomass by consumption of some organic matter over various timeframes from days to weeks (Bižić-Ionescu et al., 2018).

TEP are ubiquitous in the oceans (Passow, 2002), likely caused by abiotic coagulation and aggradation of dissolved carbohydrates or primarily acidic polysaccharides, but also by biotic formation as extracellular secretions by algae or bacteria (Chin et al., 1998; Stoderegger and Herndl, 2001; Passow et al., 2001; Berman and Viner-Mozzini, 2001; Passow et al., 1994). Particulate TEP (p-TEP) is in the size range 0.4−200 µm, with a number of forms, including amorphous blobs, disseminated clouds, sheets, filaments or clumps (Zhou et al., 1998; Passow, 2002; Mari et al., 2004). Colloidal TEP (c-TEP) consist of particles that are stained by Alcian blue

64 with a diameter range of 0.05 to 0.4 µm (Villacorte al., 2009). However, c-TEP is defined based
65 solely on staining with Alcian blue, which is known to also stain other substances in seawater,
66 including sulfated and carboxylated polysaccharides, glycoproteins, polyanions in general, and
67 acidic polysaccharides not associated with TEP (Winters et al., 2016).

68 TEP are composed of acidic polysaccharides enriched with fucose and rhamnose, thus
69 serving as a food source in the water column and commonly associated with layers of intense
70 microbial and biochemical activity (Azam and Long, 2001). TEP generally decrease in
71 concentration with depth in the sea (Engel et al., 2004), with a tendency to float to the sea
72 surface if unballasted to contribute a gelatinous layer to the sea surface microlayer (Azetsu-
73 Scott and Passow, 2004; Wurl and Holmes, 2008; Wurl et al., 2009). Bar-Zeev et al. (2015) have
74 documented that p-TEP is mainly composed of polysaccharides, which can be dispersed in the
75 presence of different types of chelators, be fractured to form colloids or reassemble abiotically.
76 The trends in TEP concentrations in the seawater column have been previously examined
77 (Jennings et al., 2017), and the relationship of TEP with TOC, DOC, and bacteria have also been
78 investigated in many areas of the ocean (Engel, 2004; Simon et al., 2002; Ortega-Retuerta et al,
79 2009; Ortega-Retuerta et al., 2011; Bar-Zeev et al., 2011). However, these relationships have
80 not been studied in the Red Sea.

81 Studies on TEP distribution in relation to other forms of organic matter in the Red Sea have
82 focused mainly on assessing the links between TEP and phytoplankton and bacterial production
83 (Bar-Zeev et al., 2009b) and the impacts of TEP and dissolved forms of NOM on biofouling in
84 seawater desalination plants (Bar-Zeev et al., 2009a; Dehwah et al., 2015a; Dehwah et al.,
85 2015b; Dehwah et al., 2015c; Dehwah and Missimer, 2016; Rachman et al., 2014; Rachman et

al., 2015). The intakes for reverse osmosis seawater desalination plants are located in shallow, nearshore areas of the Red Sea, so little consideration has been given to changes in TEP concentration with depth until it was suggested that deep-water intake systems may produce seawater quality with lower concentrations of algae, bacteria, and organic compounds, such as TEP, thus possibly lessening rates of membrane biofouling (Dehwah et al., 2015c).

The relationships between TEP concentrations and abundance of microalgae, bacteria, TOC, and dissolved fractions of NOM, including biopolymers, humic substances, building blocks, low molecular weight (LMW) acids, and LMW neutrals from the sea surface to 300 m depth are herein presented.

The present study provides the first data from the Red Sea, with initial insights into the vertical transport of organic carbon, including the fractions of natural organic matter from the surface to depths near or below the photic zone. The authors are keenly aware that the data presented herein have not been collected in a systematic manner with spatial and temporal comparisons to assess the biogeochemical cycles within the Red Sea comprehensively. However, the compiled data can be used to better characterize the biogeochemical cycles of the Red Sea as other researchers add new data. The reported datasets represent the first measured in the Red Sea wherein the fractions of organic matter, including biopolymers, humic substances, building blocks, low molecular weight neutrals, and low molecular weight acids (very expensive to measure), are linked with measurements of algae, bacteria, TOC, and TEP.

2 Methods

Biogeosciences Discuss., https://doi.org/10.5194/bg-2019-59
Manuscript under review for journal Biogeosciences
Discussion started: 13 March 2019

2.1 Compilation and comparison of available data

There have been several investigations on organic matter, including TEP, collected at depths near the sea surface along the Red Sea coast of Saudi Arabia, with the main focus to establish the relationships between seawater organic matter content and the potential for membrane biofouling in seawater desalination facilities. These shallow nearshore data were compiled and assessed to compare to the newly collected offshore data and to assess statistical relationships between various organic parameters. Note that these data have been collected at many different times of the year and were not used to attempt the characterize the natural seasonal variations and the overall biochemical activity in the nearshore area of the Red Sea.

2.2 Seawater vertical profiles in the Red Sea

Seawater properties of the water column were measured at four sites (A–D) north of Jeddah, along the Saudi coast of the Red Sea in deep water areas (> 1000 m) (Fig 1). In situ vertical profiles of temperature, salinity, dissolved oxygen (DO), pH, turbidity, chlorophyll-a (fluorescence), and photosynthetically active radiation (PAR) were determined with a multi-sensor assembly fitted to a Rosette carousel holding a set of Niskin water sampling bottles (General Oceanics, USA). Continuous vertical profiling was conducted from sea surface to 90 m depth at sites A–C, with seawater samples obtained at 10 m depth intervals for the analysis of organic parameters. At site D, continuous vertical profiles of physicochemical parameters were taken from 7 m below sea surface to 300 m depth, with seawater samples for organic

parameters obtained at 10 m intervals from the surface to 100 m depth and at 20 m intervals thereafter to 300 m depth. Sampling at sites A−C was conducted in April 2014, whereas at site D in February 2015. The sample timing was based on ship availability and the data collected cannot be used to fully characterize the Red Sea in deep water located far from the coast. Note that the water depth drops almost vertically to greater than 1000 m beginning in the nearshore at the 20 m contour (Dehwah et al., 2015c).

The multi-sensor assembly included the SBE 43 CTD device (Sea-Bird Scientific) for salinity, temperature and depth profiling, with a DO add-on sensor; Wet Labs ECO AFL/FL (Sea-Bird Scientific) was used for turbidity and fluorescence detection; and a biospherical light sensor (LI-COR) was used for PAR measurement. All sensors were pre-calibrated according to manufacturer specifications before actual use in field sampling and was normalized.

2.3 Quantification and characterization of microalgae and bacteria

Microalgal abundances in water samples were determined by flow cytometry, using a BD FACSVerse flow cytometer for counting and characterizing algal cells. An Accuri flow cytometer was used to measure bacterial abundance. Flow cytometry enables a rapid and accurate counting of microorganisms (VivesRego et al., 2000).

Light scattering properties and/or fluorescence intensity was determined by the flow cytometer to distinguish between different algal types, as described by van der Merwe et al. (2014). Lasers were used to excite both unstained autofluorescent organisms (algae) and stained bacterial cells. The red laser wavelength was set at 640 nm and the blue laser at 488 nm

for the Accuri flow cytometer. Algal cell counting was performed by combining 500 µL of each sample with a 1 µL volume of a standard containing 1 µm beads to calibrate size in a 10 mL tube. The tube was then vortexed and measured at high flow rate with a 200 µL injection volume for 2 min. The counting procedure was repeated three times to assess the precision of measurements. There different type of algae, cyanobacteria, *Prochlorococcus*, and pico/nanoplankton, were distinguished based on their autofluorescence as well as by the cell side-angle scatter, which was used to identify them by size (Radíc et al., 2009).

A comparative protocol employing SYBR®Green stain was used for bacteria counting. A volume of 500 µL from each sample was transferred to a 10 mL tube, incubated in 35°C water bath for 10 min. SYBR® Green dye was added at a 5 µL into a 500 µL aliquot to stain the cells. The sample was vortexed and incubated for 10 min. The prepared samples were then analyzed at a medium flow setting with a 50 µL injection volume for 1 min. For validation, 8-Peak calibration beads were used. Triplicate measurements were made on each sample to assess measurement precision.

2.4 Measurement of TOC and NOM fractions

TOC concentration was measured with a Shimadzu TOC-VCSH. Fractions of dissolved organic carbon, including biopolymers, humic substances, building blocks, low molecular weight (LMW) neutrals, and low molecular weight (LMW) acids, were determined by Liquid Chromatography Organic Carbon Detector (LCOCD, DOC-Labor), using a size exclusion chromatography column Toyopearl HW-50S (TOSOH), following the methods by Huber et al. (2011). A calibration curve

Biogeosciences Discuss., https://doi.org/10.5194/bg-2019-59
Manuscript under review for journal Biogeosciences
Discussion started: 13 March 2019

was established for both molecular masses of humic substances and detector sensitivity before sample measurements. Humic acid and fulvic acid standards (Suwannee River Standard II) were used for the molecular mass calibration, whereas potassium hydrogen phthalate and potassium nitrate (KNO_3) for sensitivity calibration based on Huber et al. (2011).

All seawater samples for LCOCD were manually pre-filtered using a 0.45 µm syringe filter to exclude the undissolved particulate organics. Before sample analysis, a system cleaning was performed by injection of 4,000 µL of 0.1mol/L NaOH through the column for 260 min. After cleaning, 2,000 µL of the sample was injected for analysis at 180 min retention time and 1.5 mL/min flow rate. A mobile phase of phosphate buffer, with 28 mmol STD and 6.58 pH, was used to carry the sample through the system. The resulting chromatogram showed a plot of signal response of different organic fractions against retention time. Manual integration of the data, also following Huber et al. (2011), was performed to determine the concentrations of the different organic fractions, including biopolymers, humic substances, building blocks, LMW acids and LMW neutrals.

2.5 TEP measurement

Both p-TEP and c-TEP were simultaneously determined in each collected sample. The size range of p-TEP is between 0.4 and 200 µm, whereas c-TEP between 0.05 and 0.40 µm (Villacorte et al., 2009). TEP analysis was based on the method developed by Passow and Alldredge (1995), which involves sample filtration, membrane staining with Alcian blue, and then UV spectrometry. A staining solution was prepared from 0.06% (m/v) Alcian blue 8GX (Fluka) in

acetate buffer solution (pH 4) and freshly pre-filtered through a 0.2 µm polycarbonate filter before usage. A 300 mL volume of seawater from each water sample was filtered through a 0.4 µm pore size polycarbonate membrane using an adjustable vacuum pump at low constant vacuum. After filtration, the membrane was rinsed with 10 mL of Milli-Q water to prevent the Alcian blue from coagulating, as salts may remain on the filter after seawater filtration, thus avoiding the likelihood of overestimating the TEP concentration. The retained TEP particles on the membrane surface were then stained with the Alcian blue dye for 10 seconds. After staining, the membrane was flushed with 10 mL of Milli-Q water to remove any excess dye. The flushed membrane was then placed into a small beaker, where it was soaked in 80% sulfuric acid for 6 hours to extract the dye that was bound to the p-TEP. Finally, the absorbance of the acid solution was measured by a UV spectrometer at 752 nm wavelength to determine the TEP concentration. The same methodology was applied to determine the colloidal TEP, except that a 250 ml volume of water sample from 0.4 µm polycarbonate membrane permeate was filtered through a 0.1 µm pore size to allow deposition of the c-TEP on the membrane surface.

To relate the measured UV absorbance values to TEP concentrations, a calibration curve was established. Xanthan gum solutions with different volumes (0, 0.5, 1, 2, 3 mL) were used to obtain the calibration curve (Fig. 2). The TOC concentrations of xanthan gum before and after 0.4 µm filtration were analyzed, and the TOC concentration difference was used to calculate the gum mass on each filter and the TEP concentration was estimated using the calibration curve. The same procedures were used for the 0.1 µm membrane to establish the calibration curve for colloidal particles. Afterwards, the TEP concentration was expressed in terms of Xanthan Gum equivalent in µg Xeq./L by dividing the TEP mass by the corresponding volume of

TEP samples. Because particulate and colloidal TEP is determined indirectly, these values must be considered to be semi-quantitative. The new method developed by Villacorte et al. (2009) for TEP measurement was not used, as it would limit the comparability of the measured data with previous results.

2.6 Statistical methods used for data comparison

A series of scatter plots were constructed to test the statistical significance between various organic parameters. The R^2 and p-values were calculated to assess the degree of fit to a curve and the statistical significance. When the p value was below 0.05, the null hypothesis was void and the relationship was deemed to be significant.

3 Results

3.1 Variations in salinity, temperature, fluorescence, pH, dissolved oxygen, PAR/irradiance, biospherical/licor, and turbidity

The thermocline in the three profiles (sites A-C) collected to a 90 m depth showed a slight decrease in temperature from near 29 °C to between 24 and 25 °C 90 m below surface (Fig. 3). The decline in temperature was relatively gradual at all three sites. In the deep profile, the temperature declined from about 26.5 °C at the surface to about 22 °C at 300 m. An inflection point occurred at about 115 m and the change in temperature below this depth to 300 m was only about 2.5 °C (Fig. 4). The difference in the temperature at the sea surface between profiles

was likely caused by the time of year of measurements, with the 90 m profiles occurring in April versus the 300 m profile in February which is the peak of winter in the study area.

The halocline showed similar salinity variations in the 90 m profiles with a slight, rather uniform increase from about 39 ppt at surface to 40 ppt at 90 m (Fig. 3). A slightly lower salinity gradient coinciding with a slightly higher temperature gradient occurred at site B. The salinity change in the 300 m profile showed a similar pattern from about 39 to 40 ppt in the upper 115 m, but an inflection occurred at about 115 m wherein the rate of increase declined to a few tenths of a ppt over the lower 185 m. The inflection point showing a slope change for both temperature and salinity occurred at about the same depth (Figs. 3 and 4).

The vertical trends in pH also exhibited minimal variations down to 90 m at sites A–C (Fig. 3), but with slightly lower pH values at site A (7.9–8.0) than at sites B and C (8.0–8.1). In the deep profile, pH was nearly stable at about 8.3 until 115 m and then steadily decreased to 8.1 at 300 m (Fig. 4).

Dissolved oxygen (DO) concentrations in the shallow profiles at all three sites showed high variability (6–12.5 mg/L) in the top layer (unknown reason for variation), but with relative stability at about 5 mg/L from 20 to 90 m (Fig. 3). DO in the deep profile was at lower concentrations (0.8–1.5 mg/L) near the surface, increasing to around 2 mg/L at 115 m and then steadily declined to about 0.6 mg/L at 300 m with a saturation of only 10%.

The vertical pattern in chlorophyll *a* (chl-*a*) concentrations markedly differed between shallow and deep profiles (Figs. 3 and 4). At sites A–C, chl-*a* was slightly detected at the surface but abruptly increased from 0.3 to 1.2 mg/m^3 within 50–75 m and thereafter declined to near 0.2 mg/m^3 at sites A and C and to about 0.5 mg/m^3 at site B. Chl-*a* concentrations were

262 relatively low in the deep profile, decreasing from about 0.45 mg/m^3 at the surface to about
263 0.06 mg/m^3 at 100 m, from which it remained unchanged until 300 m. Note that these chl-*a*
264 concentrations were based on *in situ* fluorescence detection using a sensor that was pre-
265 calibrated with a chlorophyll standard from the manufacturer (Wet Labs). As chlorophyll
266 fluorescence may vary with cell physiological condition, time of day, light regime, and other
267 factors, and since the sensor was not field-validated after calibration, the present chl-*a* values
268 should thus be considered semi-quantitative.

269 PAR levels at sites B and C were initially recorded at 600-700 µmol/m^2/s at the surface and
270 then steeply decreased to 120-160 µmol/m^2/s at 20 m depth, from where it further decreased
271 gradually until 90 m depth (Fig. 3). At site A, where the measurement was done at an earlier
272 time, PAR varied between 220-300 µmol/m^2/s within the top 10 m layer and then coincided
273 with the same values at sites B and C. PAR in the deep profile steeply declined from about 240
274 µmol/m^2/s near the surface to about 20 µmol/m^2/s at 40 m depth, after which it gradually
275 decreased to near zero at about 75 m depth, which is generally similar to the trend in the
276 shallow profiles (Figs. 3 and 4). The depths at which the PAR levels were at 1% of the surface
277 values were in range of 38−54 m for all sites.

278 Turbidity was generally low in the vertical profiles at all sites. Turbidity varied in the narrow
279 range of 0.2-0.3 NTU, with only a few spikes up to 0.4 NTU, in all three shallow profiles (Fig. 3).
280 In the deep profile, most turbidity values were within 0.1−0.15 NTU, with intermittent spikes up
281 to 0.2 NTU below 75 m depth (Fig. 4).

282

283 3.2 Algae and cyanobacteria concentrations

Biogeosciences Discuss., https://doi.org/10.5194/bg-2019-59
Manuscript under review for journal Biogeosciences
Discussion started: 13 March 2019

284

285 Total concentrations of algae and cyanobacteria (summed) with depth at the shallow and deep
286 sampling stations are shown in Figs. 5 and 6, respectively. Previous results on total algal and
287 cyanobacterial abundances, all collected from surface layers close to shore in the same study
288 area, are compiled in Table 1, with a range of 1,677−137,363 cells/mL (mean 44,383 cells/mL
289 out of 38 samples). Total algal and cyanobacterial concentrations from the surface at the
290 shallow stations (A−C) during the present study were comparable to the mean of the previous
291 data, while the surface concentration at the deep station (D) was close to the reported
292 maximum (Figs. 5 and 6, Table 1).

293 The vertical profiles of algal and cyanobacteria concentrations by group (cyanobacteria,
294 *Prochlorococcus* and pico/nanoplankton) are shown in Figs. 5 and 6 for the shallow (A-C) and
295 deep sites, respectively. At sites A-C, cyanobacteria were more abundant near the surface (top
296 10 m layer), below that *Prochlorococcus* was more predominant, with peak concentrations at
297 about 50 m (Fig. 5). In general, algal and cyanobacterial concentrations showed a substantial
298 decline below 80 m at all sites. The same compositional and abundance trends were exhibited
299 in the deep profile, except that cyanobacteria had higher concentrations near the surface in the
300 deep profile while *Prochlorococcus* was relatively denser at subsurface depths in the shallow
301 profiles (Fig. 6). In addition, the concentrations of pico/nanoplankton in the upper layers were
302 relatively higher at the deep site compared to the shallow sites (A-C) (Figs. 5 and 6).

303

304 3.3 Bacteria concentrations

305

306 The vertical trends in bacterial concentrations during the present study are shown in Figs. 7 and
307 8, indicating higher cell densities in the upper 50 m layer at the deep site compared to sites
308 A–C. Previous results on nearshore bacterial concentrations from the same study area ranged
309 from 1.13 x 10^5 to 2.18 x 10^6 cells mL^{-1} (mean 5.26 x 10^5 cells mL^{-1}; 40 samples) (Table 1). The
310 new data on offshore surface concentrations of bacteria are comparable to the average of the
311 nearshore results (Table 1, Figs. 7 and 8). Bacterial abundance generally declined with depth,
312 with a decrement of about 4.00 x 10^5 to 9.00 x 10^4 cells mL^{-1} from the surface to 90 m depth at
313 sites A–C (Fig. 7) and from about 5.00 x 10^5 cells mL^{-1} at the surface to 1.60 x 10^5 cells mL^{-1} at
314 160 m and to 1.00 x 10^5 cells mL^{-1} at 300 m (Fig. 8).
315
316 3.4 Total organic carbon (TOC)
317
318 TOC concentrations exhibited only minor differences between the sites, with fluctuations
319 within a narrow range in the upper 50 m layer at both the shallow and deep sites (Figs. 7 and 8).
320 Nearshore data on TOC ranged from 0.83 to 1.42 mg/L, with an average of 1.0 mg/L from 42
321 measurements (Table 1). In the offshore near-surface profiles, the TOC ranged from 0.99 to
322 1.35 mg/L.
323 TOC generally declined with depth at all sites, although only within a narrow range at sites
324 A–C between 1.2 mg/L at surface and 0.9 mg/L at 90 m depth. The decline in the deeper profile
325 was from 1.1 mg/L at surface to 1.0 mg/L at 120 m and then to 0.75 mg/L at 300 m.
326
327 3.5 Particulate and colloidal TEP concentrations

328

329 Nearshore p-TEP and c-TEP showed considerable variation in concentrations with ranges of
330 53−347 (mean 191) and 36−287 (125) µg Xeq./L, respectively (Table 1). Comparable ranges of
331 concentration for both parameters were found offshore, except for the markedly higher c-TEP
332 concentrations in the vertical profile at site A (Figs. 7 and 8).

333 Both p-TEP and c-TEP generally declined with depth, although with fluctuations between
334 50−100 m depth and an elevated value at 200 m depth in the deep profile. The difference in
335 concentrations was more pronounced for c-TEP in the deep profile, from 265 µg Xeq./L at 10 m
336 to about 70 µg Xeq./L at 300 m. The change in concentration of p-TEP with depth in the deep
337 profile was relatively slight, from about 285 µg Xeq./L at 40 m to 170 µg Xeq./L at 300 m. At the
338 shallow sites, both p-TEP and c-TEP trends with depth showed similar patterns between sites B
339 and C, except that c-TEP was unusually low in the surface layer at site C (Fig. 7).

340

341 3.6 NOM fractions

342

343 There was considerable variability in concentrations of the NOM factions in nearshore seawater
344 The range in concentration, number of samples, and average of the concentrations are the
345 following: biopolymers (28-164 µg/L, 42, 62 µg/L), humic substances (159-442 µg/L, 42, 248
346 µg/L), building blocks (81-260 µg/L, 42, 118 µg/L), LMW neutrals (16-477 µg/L, 42, 271 µg/L),
347 and LMW acids (10-130 µg/L, 42, 40 µg/L). The range in biopolymer concentrations in the
348 surface offshore samples are similar to the nearshore samples. All of the NOM fractions have
349 higher concentrations at the A, B, and C profiles compared to the deep profile.

Biogeosciences Discuss., https://doi.org/10.5194/bg-2019-59
Manuscript under review for journal Biogeosciences
Discussion started: 13 March 2019

The biopolymer fraction of NOM shows a general reduction with depth in all offshore profiles. At sites A and B there is a spike in biopolymers at 10 m with minor variation between 10 m to 90 m. In the deeper profile, there is considerable variation in the photic zone with the surface having the highest value and subsequent spikes occurring at 30 and 60 m. Beginning at about 90 m, there is a constant downward trend in concentration.

Humic acid concentrations showed only minor variations with depth in the shallow profiles, but the deep profile showed a reduction by about 29% from 90 to 300 m depth. There is a general decreasing trend in concentration of building blocks with depth at the deep site and only minimal differences throughout the depth profiles at sites A–C (Figs. 7 and 8). The concentrations of LMW neutrals at the shallow sites were the highest amongst NOM fractions, although with a wide range of variation. In contrast, LMW acids had the lowest concentrations without marked discrepancies in concentration in the vertical profiles between sites A–C, but a general reduction occurred below 120 m in the deep profile (Figs. 7 and 8).

4 Discussion

4.1 Algal and cyanobacterial concentrations

The flow cytometry approach used in this study was highly effective in characterizing and enumerating the small size classes of phytoplankton and cyanobacteria that are readily distinguishable on the basis of cell size and autofluorescence. Thus, cyanobacteria (presumably *Synechococcus* spp), *Prochlorococcus*, and the general class of pico/nanoplankton were

numerically dominant, with very few larger eukaryotic algal species detected. This is consistent with prior studies that reported that phytoplankton in the oligotrophic northern Red Sea and Gulf of Aqaba are dominated (>95%) by cells <5 µm in size (Lindell and Post 1995; Yahel et al. 1998). Only during the summer does the large macroalgae *Trichodesmium* sp. also become prominent. As reported here, algae ranging from 5 to several hundred µm are extremely scarce, although not totally absent (Sommer 2000; Kimor and Goldanski 1992).

4.2 Correlations between TEP, bacteria, algae, the biopolymer fraction of NOM, and TOC

TEP is composed of acidic polysaccharides and some large proteins that occur mostly in the biopolymer fraction of NOM and some of the proteins within the humic acid part of NOM (Bar-Zeev et al. 2015; Winters et al. 2016). TEP can be produced both abiotically and as extracellular discharges from bacteria and algae (Zhou et al. 1998; Passow et al. 2001; Passow 2002; Engel et al. 2004; Iuculano et al. 2017). Therefore, there should be some statistical relationship between TEP, the biopolymer fraction of NOM, bacterial concentration or algal concentration.

A series of statistical analyses were preformed to test if there are significant relationships between the various organic properties (Table 2). In all cases there was no statistically-significant relationship between any of these parameters in the shallow, nearshore samples with the exception of bacteria and TOC. However, some important and statistically-significant relations were found between p-TEP and bacteria in the profiles measured at sites A, B, and C and in the 300 m profile. All of the offshore profiles showed a statistically significant relationship between c-TEP and bacteria with the exception of the site C profile. In comparison,

394 there was only one statically-significant relationship between p-TEP and algae at site B and for
395 c-TEP the only profile showing statistical-significance was the deep profile. Based on these
396 relationships, it appears that p-TEP may be produced by bacteria in greater amounts compared
397 to algae at these locations. Consumption of the TEP by bacteria does not seem to be occurring
398 in the water column at sites A, B, and C based on the p-TEP relationship, unless abiotically-
399 generated p-TEP is replacing what is consumed. In the deep profile, the c-TEP concentration
400 shows a statistically-significant relationship with bacteria which could indicate a breakdown of
401 the p-TEP, particularly outside of the photic zone.

402 The relationship between the biopolymers and bacterial concentrations shows a significant
403 statistical correlation in all offshore profiles while the correlation between biopolymers and
404 algal concentrations is statistically significant only at site A and in the deep profile. These
405 relationships suggest that extracellular discharges of polysaccharides and proteins from the
406 bacteria and algae are occurring without immediate abiotic assembly into p-TEP. This
407 suggestion is further supported by the statistical relationships between biopolymers and p-TEP
408 and c-TEP which are statistically significant at several, but not all of the offshore profiles.

409 The offshore profiles show statistically-significant relationships between both p-TEP and c-
410 TEP and TOC at sites A and the deep profile. Therefore, TEP in general is a significant part of
411 TOC in the Red Sea at these locations, particularly below the photic zone.

412 There is usually no statistical relationship of significance between p-TEP and c-TEP.
413 However, at site A the data produced an r^2 value of 1 and with a corresponding p-value of 0
414 (Table 2). This unusual relationship has no explanation but is noted.

A considerable amount of additional research will be required to better establish the processes occurring within the Red Sea water column that relate to NOM production and transport and how these processes relate to the measured TEP and NOM fraction concentrations. Since there are few data available in the literature that relate these parameters within the water column at other geographic locations, it is difficult to provide definitive conclusions. The data provided here appear to be the first published that relate the biopolymer fraction of NOM to TEP and provide all of the five fractions of NOM in the offshore marine environment throughout the water column. The carbon compounds that occur in p-TEP are largely contained within the biopolymer fraction of NOM with the exception of some proteins which occur in the size range found in the humic substances.

An assessment of the other fractions of NOM, humic substances, building blocks, LWM neutrals, and LMW acids, did not show any significant statistical relationships between these parameters, nor did it reveal potential relationships between them and the bacteria or algae.

4.3 Comparison of the offshore and onshore TEP data in the Red Sea

All of the onshore measurements of p-TEP and c-TEP were collected between the sea surface and a depth of 10 m. Therefore, only the data in this depth range can be compared to the offshore data. The full range of p-TEP in the nearshore measurements is from 53 to 347 µg Xeq./L and the c-TEP range is between 36 and 287 µg Xeq./L. The ranges in the offshore profiles in the same depth range for p-TEP and c-TEP are 135.4 to 279.4 and 0 to 340.7 respectively. In both locations there was considerable variation between sites and in different times of the year

437 which is expected based on production variations of TEP by algae and bacteria in the upper
438 photic zone as well as the ability of TEP to have either negative or positive buoyancy at shallow
439 depths (Zhou et al., 1998; Passow, 2002; Mari et al., 2004; Schuster and Herndl 1995; Ortega-
440 Retuerta et al. 2017).

441

442 4.4 Comparison of TEP profiles in the Red Sea with other marine environments

443

444 Most TEP data profiles collected in the marine environment show an irregular variation in the
445 upper 100 m of the water column (Schuster and Herndl 1995; Ortega-Retuerta et al. 2017), a
446 general reduction of TEP with depth over 200 m (Busch et al. 2017; Jennings et al. 2017), but in
447 some cases an increase at greater depths (Ramaiah et al., 2000). Also, the reported changes in
448 TEP with depth are based mostly on p-TEP data and not both types of TEP which show differing
449 trends in the water column. The TEP data collected from the profiles in this investigation within
450 the photic zone (<100m) show differing concentrations with depth (Figs. 7 and 8). Within the
451 upper 90, p-TEP declines between 31 and 39% at sites A, B, and C and shows no decline in the
452 deep profile. The c-TEP concentration declines between 38 and 70% at sites A, B, and the deep
453 profile, but increases by 150% at site C. For comparison, the TOC concentration reduction in the
454 photic zone ranges between 10 and 32%. In the deep profile the difference between the
455 surface and the 300 m depth showed a reduction in p-TEP of 20% and c-TEP of 69%. This may
456 indicate that some abiotic assembly of p-TEP is occurring below the photic zone, particularly in
457 the presence of bacteria which may feed upon the p-TEP. The TOC in the deep profile declines
458 by about 32% comparing the surface to the 300 m depth.

459

460 4.5 Relationships between NOM fractions and other parameters

461

462 The primary fraction of NOM that shows a trend with depth is the biopolymers which track
463 well to bacteria. Since the biopolymer fraction of NOM contains most of the polysaccharides,
464 which are food for bacteria, the relationship with the bacteria is to be expected. In the upper
465 100 m of the water column, the humic substances show a restricted range in concentrations
466 with a small downward trend (Fig. 7), but below 100 m there is a lowering concentration
467 following the same pattern as the biopolymers. The building blocks have a larger range in
468 concentration changes in the upper 100 m of the water column compared to the humic
469 substances (Fig. 7) and a similar downward trend in concentration similar to the humic
470 substances below 100 m (Fig. 8). The LMW neutrals and acids show considerable variation in
471 concentration in the upper 100 m and a slight downward change in concentration below 100 m.
472 There are some general suggestions made by these data related to the concentration
473 changes. In the photic zone, the biochemical activity of algae and bacteria affect the NOM
474 fraction concentrations. The LMW fractions are likely affected by the biochemical breakdown of
475 large molecular weight organics and by selective, abiotic aggradation of larger organic particles
476 suggested by the larger concentration of the neutrals over the acids. The reduction in
477 concentrations in biopolymers, humic substances and building blocks below 100 m follows the
478 reduction in bacteria below the photic zone. As bacteria feed on p-TEP, they may leave behind
479 the LMW neutrals which could be compounds that cannot be used by the bacteria as food. The
480 LMW acids may tend to occur within the context of c-TEP and may be subject to abiotic

aggradation during settling. Future research will be required to understand the complex relations between the NOM organic fractions and the biochemistry of the bacteria in the deep-water column.

5 Conclusions

Vertical changes in concentrations of TEP in the Red Sea tend to follow trends found in other locations of the world ocean in that there is a general reduction with depth. The changes in the photic zone tend to be quite irregular, as expected, because of variations in primary productivity and differing biochemical conditions. Although it was observed that no clear relationship between TEP and algae occurs in the Red Sea, this unusual result may be explained by the dominance of small algae and cyanobacteria. The measurement of the five fractions of NOM allows some preliminary conclusions to be made concerning the relationships between specific organic parameters and TEP variation with depth. These relationships suggest that extracellular discharges of polysaccharides and proteins from the bacteria and algae are occurring without immediate abiotic assembly into p-TEP in the photic zone of the water column. In the water column below the photic zone, TOC, bacteria, and biopolymers show a generally common rate of reduction in concentration, but p-TEP concentration changes at a reduced rate showing that it persists in moving organic carbon deeper into the water column despite consumption by bacteria. There may be some abiotic assembly of c-TEP into p-TEP to maintain the concentration without full bacterial removal.

The relationships between p-TEP and c-TEP and other organic parameters, especially the biopolymer fraction of NOM, is different when comparing the offshore water column to the nearshore area. The only statistically-significant relationship in the measured parameters in the nearshore was that between bacteria and TOC. Irregularity in local conditions in the nearshore zone causes large variations in the organic parameters measured, not allowing statistically-significant relationships to be established.

References

Alldredge, A. L., and Croker, K. M.: Why do sinking mucilage aggregates accumulate in the water column?, Sci. Total Environ. 165, 15-22, 1995.

Azam, F., and Long, R. A.: Sea snow microcosms, Nature 414, 495-497, 1995.

Azam, F. and Malfatti, F.: Microbial structuring of marine ecosystems. Nature Reviews Microbiology, 5(10), 782-791, 2007.

Azetsu-Scott, K. and Passow, U.: Ascending marine particles: significance of transparent exopolymer particles (TEP) in the upper ocean, Limnol. Oceanogr. 49, 741-748, 2004.

Bar-Zeev, E., Berman, T., Rahav, E., Dishon, G., Herut, B., Kress, N. and Berman- Frank, I., 2011. Transparent exopolymer particle (TEP) dynamics in the eastern Mediterranean Sea. Marine Ecology Progress Series, 431, pp.107-118.

Bar-Zeev, E., Berman-Frank, I., Stambler, N., Domínguez, E. V., Zohary, T., Capuzzo, E. Meeder, E., Suggett, D. J., Iluz, D., Dishon, G., and Berman, T.: Transparent exopolymer particles (TEP)

link phytoplankton and bacterial production in the Gulf of Aqaba, Aquat. Microbobial Ecol. 56, 217-226, 2009a.

Bar-Zeev, E. I., Berman-Frank, I., Liberman, B., Rahav, E., Passow, U., and Berman, T.: Transparent exopolymer particles: Potential agents for organic fouling and biofilm formation in desalination and water treatment plants, Desalination and Water Treatment 3, 136-142, 2009b.

Bar-Zeev, E., Passow, U., Romero-Vargas, C. S., and Elimelech, M: Transparent exopolymer particles (TEP): from aquatic environments and engineered systems to membrane biofouling, Environ. Sci. Technol. 49(2), 691-707, 2015.

Berman, T., Viner-Mozzini. Y.: Abundance and characteristics of polysaccharide and proteinaceous particles in Lake Kinneret, Aquat. Microb. Ecol. 24, 255-264, 2001.

Bižić-Ionescu, M., Ionescu, D. and Grossart, H.P.: Organic particles: heterogeneous hubs for microbial interactions in aquatic ecosystems, Frontiers in Microbiology, 9, 2018.

Busch, K., Endreas, S., Iverson, M. H., Michels, J., Nöthig, E.-M., and Engel, A: Bacterial colonization and vertical distribution of marine gel particles (TEP and CSP) in the Arctic Fram Strait, Frontiers Mar. Sci 4, Article 166, doi:10.2289/fmars.2017.00166, 2017.

Chin, W.-C., Orellana, M. V., and Werdugo, P.: Spontaneous assembly of marine dissolved organic matter in polymer gels, Nature 391, 568-572, 1998.

Dehwah, A. H. A., Al-Mashharawi, S., Kammourie, N., and Missimer, T. M.: Impact of well intake systems on bacterial, algae and organic carbon reduction in SWRO desalination systems, SAWACO, Jeddah, Saudi Arabia, Desalination and Water Treatment 55(10), 2594-2600, 2015a.

Dehwah, A. H. A, Li, S., Al-Mashhaarwi, S., Winters, H., T. M. Missimer, T. M.: Changes in feedwater organic matter concentrations based on intake type and pretreatment processes at SWRO facilities, Red Sea, Saudi Arabia, Desalination 360, 19-27, 2015b, http://dx.doi.org/10.1016/j.desal.2015.01.008.

Dehwah, A. H. A., Li, S., Al-Mashharawi, S., Mallon, F. L., Batang, Z., and Missimer, T. M.: Effects of intake depth on raw seawater quality in the Red Sea, Chapter 6, In: Missimer, T. M., Jones, B., and Maliva R. G. [eds], Intakes and Outfalls for Seawater Reverse Osmosis Desalination Facilities: Innovations and Environmental Impacts, Springer, Berlin, p.105-124, 2015c.

Dehwah, A. H. A., and Missimer, T. M.: Subsurface intake systems: green choice for improving feed Seawater quality at SWRO desalination plants, Jeddah, Saudi Arabia, Water Research 88, 216-224, 2016.

Engel, A., 2004. Distribution of transparent exopolymer particles (TEP) in the northeast Atlantic Ocean and their potential significance for aggregation processes. Deep Sea Research Part I: Oceanographic Research Papers, 51(1), pp.83-92.

Engel, A., Thoms, S., Rieesell, U., Rochelle-Newall, E., and Zondervan, I.: Polysaccharide aggregation as a potential sink of marine dissolved organic carbon, Nature 428, 929-932, 2004.

Iuculano, F., Mazuecos, I. P., Reche, I., and Agusti, S.: *Prochlorococcus* as a possible source for transparent exopolymer particules (TEP). Front. Microbio. 8: Article 709, doi:10.3389/fmicro.2017.00709, 2017.

566 Lindell, D. and Post, A. F.: Ultraphytoplankton succession is triggered by deep winter mixing in
567 the Gulf of Aqaba (Eilat), Red Sea, Limnol. Oceanogr. 40(6), 1130-1141, 1995.
568 Mari, X., Rassoulzadegan, F., and Brussaard, C. P. D.: Role of TEP in the microbial food web
569 structure. II. Influence of the ciliate community structure, Mar. Ecol. Prog. Ser. 279, 23-32,
570 2004.
571 Ortega-Retuerta, E., Duarte, C.M. and Reche, I., 2010. Significance of bacterial activity for the
572 distribution and dynamics of transparent exopolymer particles in the Mediterranean Sea.
573 Microbial ecology, 59(4), pp.808-818.
574 Ortega-Retuerta, E., Reche, I., Pulido-Villena, E., Agustí, S. and Duarte, C.M., 2009. Uncoupled
575 distributions of transparent exopolymer particles (TEP) and dissolved carbohydrates in the
576 Southern Ocean. Marine chemistry, 115(1-2), pp.59-65.
577 Ortega-Retuerta, E., Sala, M. M., Borrull, E., Mestre, M., Aparicio, F. L., Gallisai, R., Antequera,
578 C., Marrasé, C., Peters, F., Simó, R., and Gasol, J. M.: Horizontal and vertical distributions of
579 transparent exopolymer particles (TEP) in the NW Mediterranean Sea are linked to
580 chlorophyll a and O_2 variability, Front. Microbiol. 7, article 2159,
581 doi:10.3389.fmicb.2016.02169, 2017.
582 Passow, U.: Transparent exopolymer particles (TEP) in aquatic environments, Prog. Oceanogr.
583 55, 287-333, 2002.
584 Passow, U., and Alldredge, A. L.: A dye-binding assay for spectrophotometric measurement of
585 transparent exopolymer particles (TEP), Limnol. Oceanogr. 40(7), 1326-1335, 1995.
586 Passow, U., Alldredge, A. L., and Logan, B. F.: The role of particulate carbohydrates in the
587 flocculation of diatom blooms, Deep-Sea Res. I 41, 335-357, 1994.

588 Passow, U., Shipe, R. F., Muarry, A., Pak, D. K., Brzezinski, M. A., and Alldredge, A. L.: The origin
589 of transparent exopolymer particles (TEP) and their role in the sedimentation of particulate
590 matter, Cont. Shelf Res. 21, 327-346, 2001.
591 Rachman, R. M., Li, S., and Missimer, T. M.: SWRO feed water quality improvement using
592 subsurface intakes in Oman, Spain, Turks and Caicos Islands, and Saudi Arabia, Desalination
593 351, 88-100, 2014.
594 Rachman, R., Dehwah, A. H. A., Li, S., Winters, H., Al-Mashharawi, S., and Missimer, T. M.: 2015.
595 Effects of well intake systems on removal of algae, bacteria, and natural organic matter,
596 Chapter 9, In: Missimer, T. M., Jones, B., and R. G. Maliva, R. G. (Eds.), Intakes and Outfalls
597 for Seawater Reverse Osmosis Desalination Facilities: Innovations and Environmental
598 Impacts, Springer, Berlin, pp. 163-193, 2015.
599 Radíc, T., Šilovic, T., Šantíc, D., Fuks, D., and Micić, M.: Preliminary flow cytometric analysis of
600 phototrophic pico- and nanoplankton communities in the Northern Adriatic Fresenius,
601 Environ. Bull. 18, 715-724, 2009.
602 Ramaiah, N., Sarma, V. V. S. S., Gauns, M., Dileep Kumar, M., and Madhupratap, M.: Abundance
603 and relationship of bacteria with transparent exopolymers during the 1996 summer
604 monsoon in the Arabian Sea, Proc. Indian Acad. Sci. (Earth Planet. Sci.) 109(4), 443-451,
605 2000.
606 Schuster, S., and Herndl, G. J.: Formation and significance of transparent exopolymer particles
607 in the northern Adriatic Sea, Mar. Ecol. Progr. Ser. 124, 227-236, 1995.
608 Simon, M., Grossart, H.P., Schweitzer, B. and Ploug, H., 2002. Microbial ecology of organic
609 aggregates in aquatic ecosystems. Aquatic microbial ecology, 28(2), pp.175- 211.

610 Stoderegger, K. E., and Herndl, G. J.: Production of exopolymer particles of marine
611 bacterioplankton under contrasting turbulence conditions, Mar. Ecol. Prog. Ser. 189, 9-16,
612 1999.
613 Verdugo, P., Alldredge, A. L., Azam, F., Kirchman, D. L., Passow, U., and Santschi, P. H.: The
614 oceanic gel phase: a bridge in the DOM-POM continuum, Mar. Chem. 92, 67-85, 2004.
615 Van der Merwe, R., Hammes, F., Lattemann, S., and Amy, G.: Flow cytometric assessment of
616 microbial abundance in the near-field area of seawater reverse osmosis concentrate
617 discharge, Desalination 343, 208-216, 2014.
618 Vives-Rego, Lebaron, P., and Nebe-von Caron, G.: 2000. Current and future applications of flow
619 cytometry in aquatic microbiology, FEMS Microbiol. Rev. 24(4), 429-448, 2000.
620 Winters, H., Chong, T. H., Fane, A. G., Krantz, W., Rzechowisc, M., and Saeidi, N.: The
621 involvement of lectins and lectin-like substances in biofilm formation of RO membranes – is
622 TEP important? Desalination 399: 61-68, 2016.
623 Wurl, O. L., and Holmes, M.: The gelatinous nature of the sea-surface microlayer, Mar. Chem.
624 100, 89-97, 2008.
625 Wurl, O., Miller, L., Röttgers, R., and Vagle, S.: The distribution and fate of surface-active
626 substances in the sea-surface microlayer and water column, Mar. Chem. 115, 1-9, 2009.
627 Wurl, O., Miller, L., and Vagle, S.: Production and fate of transparent exopolymer particles in
628 the ocean, J. Geophys. Res. 116, C00H13, 1-16, doi:10.1029/2011JC007342, 2011.
629 Yahel, G., Post, A. F., Fabricius, K., Marie, D., Vaulot, D., and Genin, A.: Phytoplankton
630 distribution and grazing near coral reefs, Limnol. Oceanogr. 43(4), 551-563, 1998.

Biogeosciences Discuss., https://doi.org/10.5194/bg-2019-59
Manuscript under review for journal Biogeosciences
Discussion started: 13 March 2019

631 Zhou, J., Mopper, K., and Passow, U.: The role of surface-active carbohydrates in the formation
632 of transparent exopolymer particulates by bubble adsorption of seawater, Limnol.
633 Oceanogr. 43, 1860-1871, 1998.

634

635 Table 1. Compilation of related data from previous studies

636

Location	Date	Depth (m)	Total Algae (cells/mL)	Bacteria (cells/mL)	TOC (mg/L)	NOM (µg/L)			
						Biopoly.	Humic substances	Building Blocks	LMWN
[1]N. Obhor	1/8/2014	Surface	30,524	112,790	0.89	76	345	103	168
[1]Corniche	1/11/2014	Surface	3,603	196,377	0.94	90	360	91	192
[1]S. Jeddah	1/9/2014	Surface	1,677	264,728	1.02	116	351	139	197
[1]Buhayrat	-	Surface	30,395	320,870	1.053	47	343	82	16
[2]Site A (Buhayrat)	1/7/2014	Surface	14,956	179,837	0.88	63	367	131	230
[2]Site B (Saudia)	5/25/2013	Surface	23,773	317,174	0.83	84	289	101	45
[3]N. Obhor	10/25/2014	Surface	129,738	520,350	1.1	57	205	95	163
[3]Corniche	11/6/2014	Surface	89,033	254,450	1.0	44	201	86	249
[3]S. Jeddah	12/24/2014	Surface	42,923	216,400	0.9	32	196	95	276
[4]N. Obhor	6/7/2015	Surface	-	707,100	1.262	40	194	85	466
[4]N. Obhor	6/17/2015	Surface	-	-	1.034	42	185	99	231
[4]N. Obhor	7/1/2015	Surface	108,740	282,450	1.162	49	192	105	313
[4]N. Obhor	7/12/2015	Surface	87,615	252,233	1.036	50	188	105	477
[4]N. Obhor	8/3/2015	Surface	135,603	908,100	1.104	80	209	122	269
[4]N. Obhor	8/16/2015	Surface	49,770	1,764,850	1.118	71	184	111	284
[4]Saudia	6/7/2015	Surface	-	317,567	1.055	29	172	100	369
[4]Saudia	6/17/2015	Surface	-	-	1.233	46	189	84	183
[4]Saudia	7/1/2015	Surface	61,925	583,400	1.287	44	190	93	152
[4]Saudia	7/12/2015	Surface	137,363	1,070,400	1.294	40	159	82	188
[4]Saudia	8/3/2015	Surface	53,810	1,736,450	1.164	93	180	111	238
[4]Saudia	8/16/2015	Surface	43,060	2,182,550	1.181	83	208	103	276
[5]N. Ohbor	2/4/2015	Surface	91,870	1,356,600	1.10	55	214	98	387
[6]KAUST SW	5/3/2014	Surface	4,766	273,400	1.42	29	217	119	315
[6]KAUST SW	5/22/2014	Surface	9,350	236,000	1.037	55	197	121	252
[6]KAUST SW	6/11/2014	Surface	3,140	287,850	0.992	36	246	81	319
[6]KAUST SW	7/3/2014	Surface	4,958	324,600	1.085	43	212	151	227
[6]KAUST SW	7/19/2014	Surface	11,080	389,450	0.97	53	212	91	233

Biogeosciences Discuss., https://doi.org/10.5194/bg-2019-59
Manuscript under review for journal Biogeosciences
Discussion started: 13 March 2019

[6]KAUST SW	8/18/2014	Surface	6,057	316,450	1.112	40	201	88	225
[6]KAUST SW	9/18/2014	Surface	52,453	321,250	0.923	35	193	93	171
[6]KAUST SW	10/21/2014	Surface	12,228	630,600	0.831	39	193	108	256
[6]KAUST SW	12/3/2-14	Surface	10,673	347,133	1.004	33	189	101	288
[6]KAUST SW	2/11/2015	Surface	12,890	292,500	1.275	36	200	102	343
[6]KAUST SW	5/21/2015	Surface	28,009	450,800	0.93	31	177	93	236
[6]KAUST SW	8/6/2015	Surface	44,153	336,900	1.041	42	184	86	229
[6]KAUST SW	9/17/2015	Surface	52,453	297,867	1.084	28	188	86	230
[7]KAUST SW	9/30/2016	Surface	11,955	369,300	1.073	112	429	213	385
[7]KAUST SW	10/2/2014	Surface	10,600	367,000	0.993	105	363	193	353
[7]KAUST SW	10/9/2014	Surface	17,777	368,463	0.944	140	373	218	335
[7]KAUST SW	10/16/2014	Surface	22,030	319,950	0.961	88	340	216	346
[7]KAUST SW	10/27/2014	Surface	42,550	297,700	0.917	164	348	260	468
[7]KAUST SW	11/6/2014	Surface	86,033	587,200	0.864	73	442	93	470
[7]KAUST SW	11/17/2014	Surface	107,030	673,700	0.897	71	374	221	352
No. Samples			38	40	42	42	42	42	42
Range in values			1,677-137,363	112,790-2,182,550	0.830-1.420	28-164	159-442	81-260	16-477
Average			44,383	525,820	1	62	248	118	271

[1] R. Rachman et al. 2015; [2] Dehwah et al. 2015; [3]Dehwah and Missimer 2016, [4]Alsahri et al. 2017,
[5]Dehwah et al 2017; [6]Dehwah and Missimer 2017; [7]Dehwah and Missimer 2015d

Table 2. Regression analysis of selected organic parameters at the 0.05 significance level

0.05 level

Organic Parameters	Location	R^2	p-value	Significant (?)
p-TEP v. Bacteria	Site A	0.6677	0.0039	Y
	Site B	0.7295	0.001656	Y
	Site C	0.6691	0.00383	Y
	Deep Profile (300 m)	0.3034	0.009661	Y
	Nearshore	0.0593	0.158757	N
p-TEP v. Algae	Site A	0.1011	0.37063	N
	Site B	0.5363	0.016017	Y
	Site C	0.2463	0.144607	N
	Deep Profile (300 m)	0.1495	0.083384	N
	Nearshore	0.0169	0.471436	N
c-TEP v. Bacteria	Site A	0.6677	0.0039	Y
	Site B	0.6430	0.005265	Y
	Site C	0.2474	0.143485	N
	Deep Profile (300 m)	0.5512	0.000116	N
	Nearshore	0.2622	0.006329	N
c-TEP v. Algae	Site A	0.1011	0.37063	N
	Site B	0.2900	0.108267	N

	Site C	0.0141	0.743804	N
	Deep Profile (300 m)	0.5713	7.4E-05	Y
	Nearshore	0.1476	0.057986	N
Biopolymers v. Bacteria	Site A	0.8166	0.000335	Y
	Site B	0.6726	0.003663	Y
	Site C	0.6868	0.003043	Y
	Deep Profile (300 m)	0.7814	1.08E-07	Y
	Nearshore	0.0123	0.495799	N
Biopolymers v. Algae	Site A	0.5801	0.010465273	Y
	Site B	0.2918	0.10701	N
	Site C	0.2996	0.101512	N
	Deep Profile (300 m)	0.7078	1.77E-06	Y
	Nearshore	0.0107	0.537011	N
Biopolymers v. p-TEP	Site A	0.4890	0.024407	Y
	Site B	0.4824	0.0258132	Y
	Site C	0.4020	0.049006	Y
	Deep Profile (300 m)	0.1551	0.077318	N
	Nearshore	0.0808	0.09790	N
Biopolymers v. c-TEP	Site A	0.4890	0.024407	Y
	Site B	0.3696	0.062253	N
	Site C	0.2590	0.13302	N
	Deep Profile (300 m)	0.5883	4.97E-05	Y
	Nearshore	0.0331	0.364097	N
p-TEP v. c-TEP	Site A	1	0	Y
	Site B	0.362578	0.065466	N
	Site C	0.3798	0.057758	N
	Deep Profile (300 m)	0.1660	0.066765	N
	Nearshore	0.0491	0.266597	N
p-TEP v. TOC	Site A	0.6591	0.00434	Y
	Site B	0.2760	0.118919	N
	Site C	0.0979	0.378796	N
	Deep Profile (300 m)	0.3156	0.008046	Y
	Nearshore	0.0284	0.332963	N
c-TEP vs. TOC	Site A	0.6591	0.0043396	Y
	Site B	0.0431	0.565154	N
	Site C	0.0165	0.723942	N
	Deep Profile (300 m)	0.6698	5.79E-06	Y
	Nearshore	0.1995	0.019513	N
Bacteria v. TOC	Site A	0.7717	0.000822	Y
	Site B	0.2994	0.101653	N
	Site C	0.1294	0.307187	N
	Deep Profile (300 m)	0.7812	1.08E-07	Y
	Nearshore	0.1144	0.032827	Y
Algae v. TOC	Site A	0.0928	0.3922134	N
	Site B	0.4907	0.024064	N
	Site C	0.3188	0.089015	N

	Deep Profile (300 m)	0.6220	2.16E-05	Y
	Nearshore	0.0388	0.236167	N

641

642 **Acknowledgments**

643

644 Funding for the offshore sample collection was provided by the King Abdullah University of
645 Science and Technology Coastal and Marine Resources Core Laboratory. Analytical work was
646 funded by the Water Desalination and Reuse Center, King Abdullah University of Science and
647 Technology. Support for DMA was provided by the National Science Foundation (Grants OCE-
648 0850421 OCE-0430724, OCE-0911031, and OCE-1314642) and National Institutes of Health (NIEHS-
649 1P50-ES021923-01) through the Woods Hole Center for Oceans and Human Health.

650

651 **Conflicts of Interest**

652 None declared

653

654 Figure captions

Biogeosciences Discuss., https://doi.org/10.5194/bg-2019-59
Manuscript under review for journal Biogeosciences
Discussion started: 13 March 2019

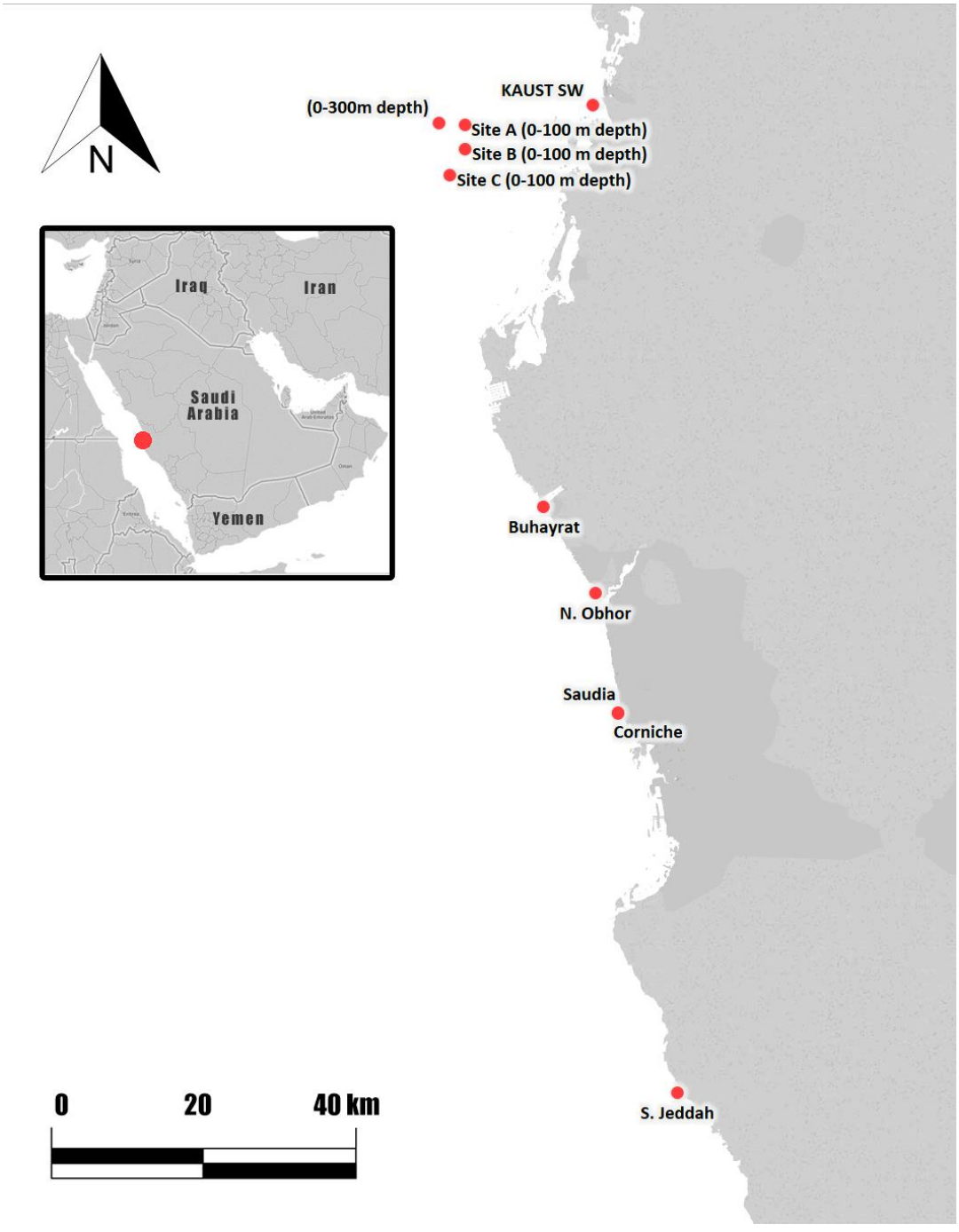

655

656 Fig. 1. Map showing the sampling profile locations in the Red Sea

Biogeosciences Discuss., https://doi.org/10.5194/bg-2019-59
Manuscript under review for journal Biogeosciences
Discussion started: 13 March 2019

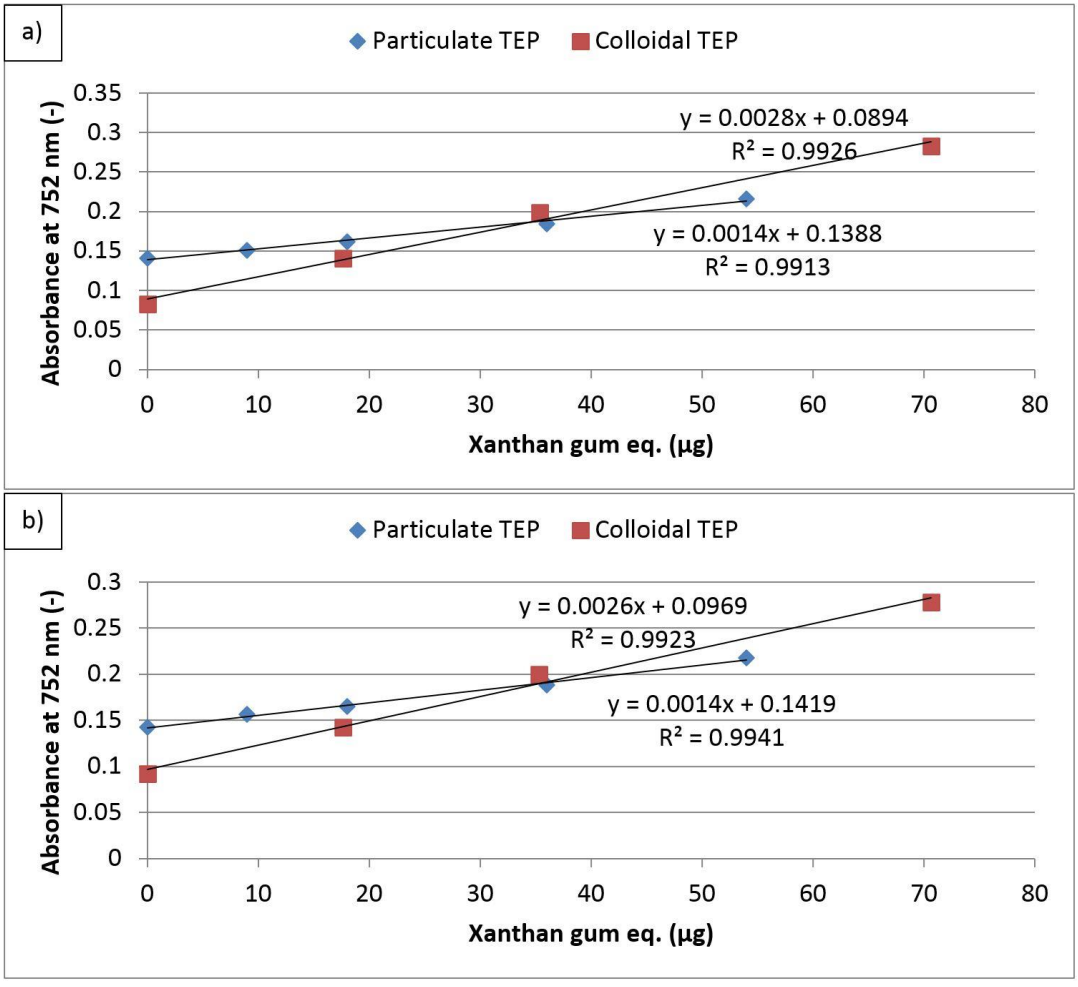

657

658 Fig. 2. Xanthan gum standard calibration curves for determination of p-TEP and c-TEP

Biogeosciences Discuss., https://doi.org/10.5194/bg-2019-59
Manuscript under review for journal Biogeosciences
Discussion started: 13 March 2019

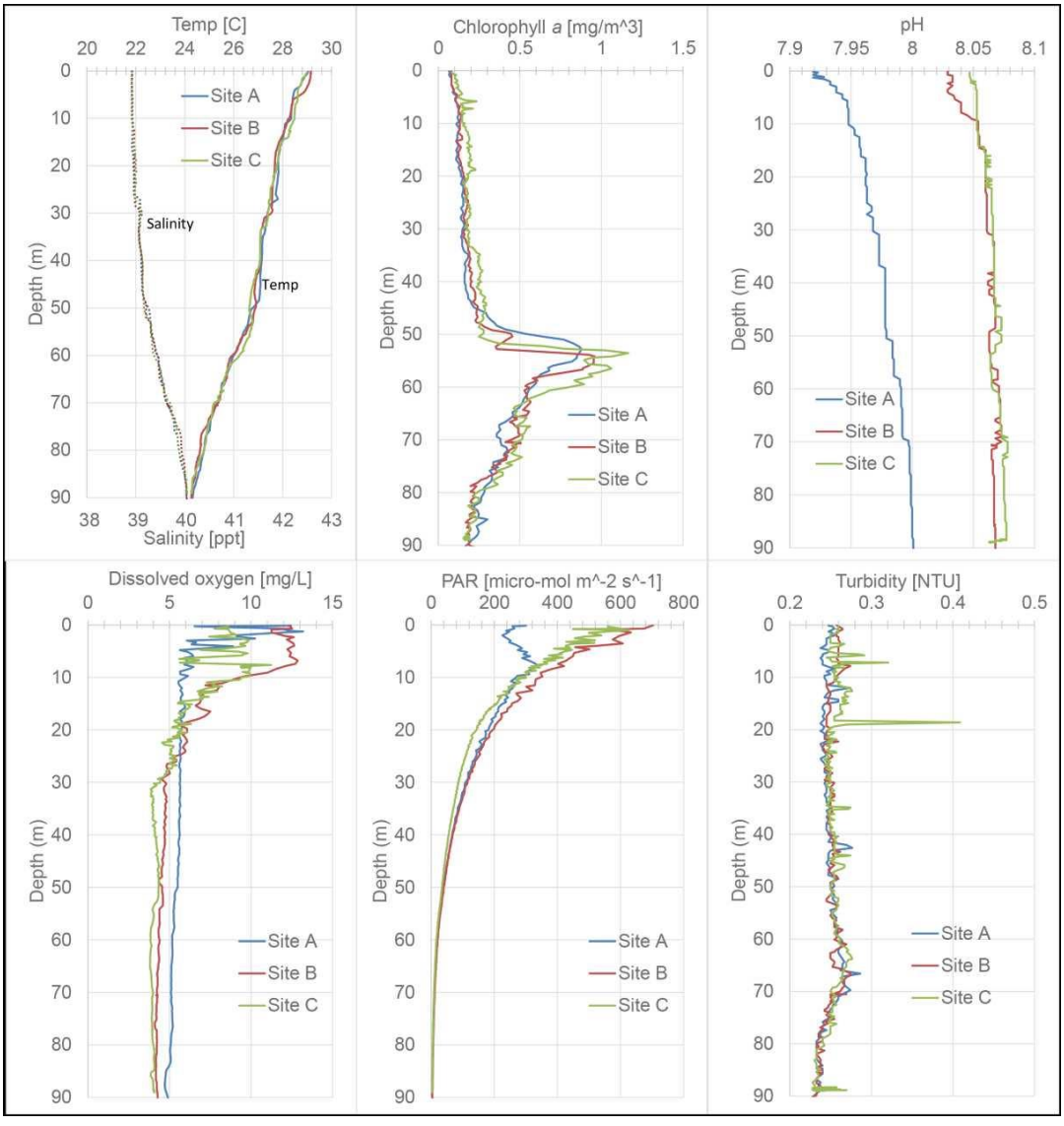

659

660 Fig. 3. Physical data from the three 90 m profiles

Biogeosciences Discuss., https://doi.org/10.5194/bg-2019-59
Manuscript under review for journal Biogeosciences
Discussion started: 13 March 2019

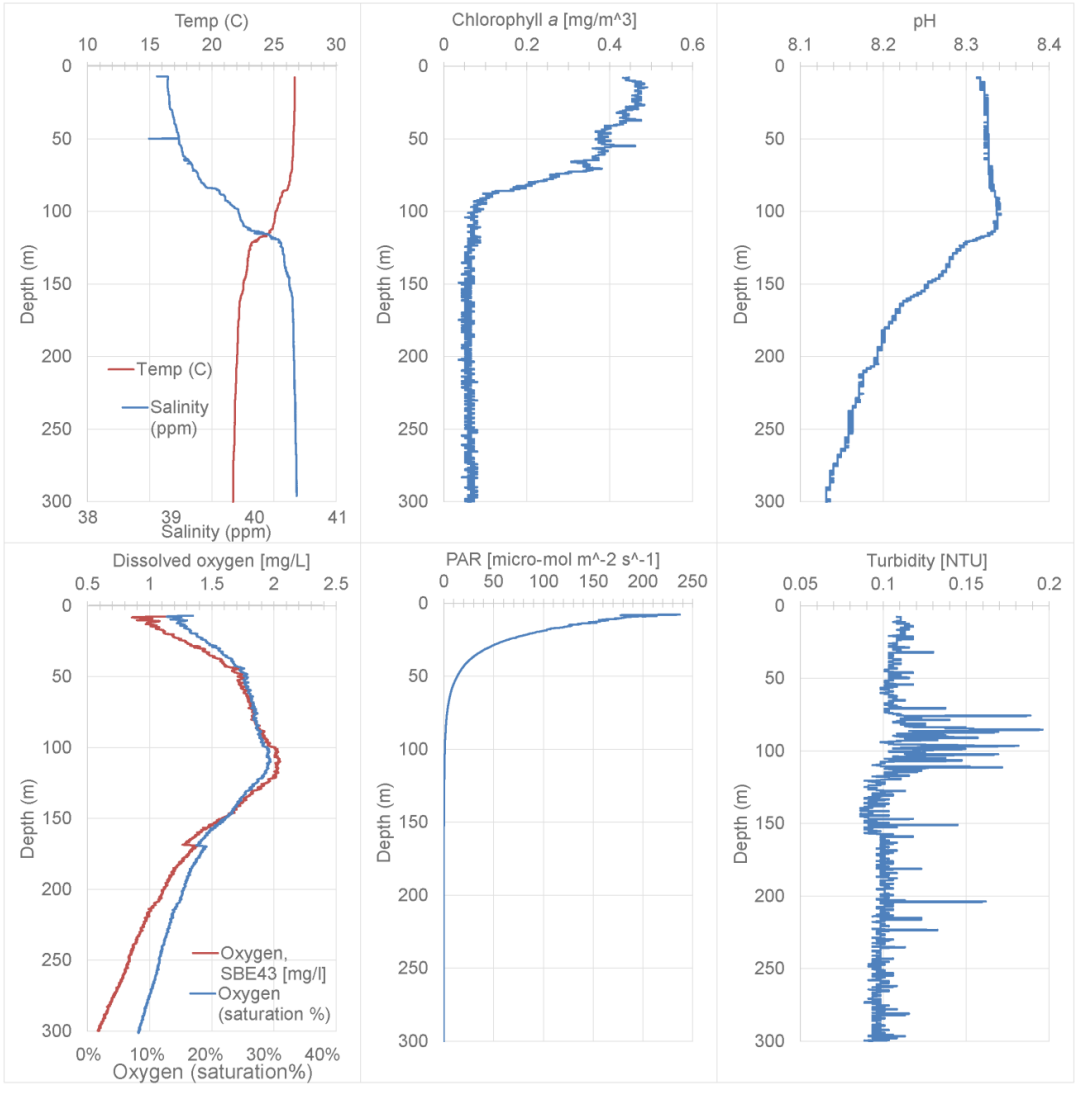

661

662 Fig. 4. Physical data from the 300 m profile

Biogeosciences Discuss., https://doi.org/10.5194/bg-2019-59
Manuscript under review for journal Biogeosciences
Discussion started: 13 March 2019

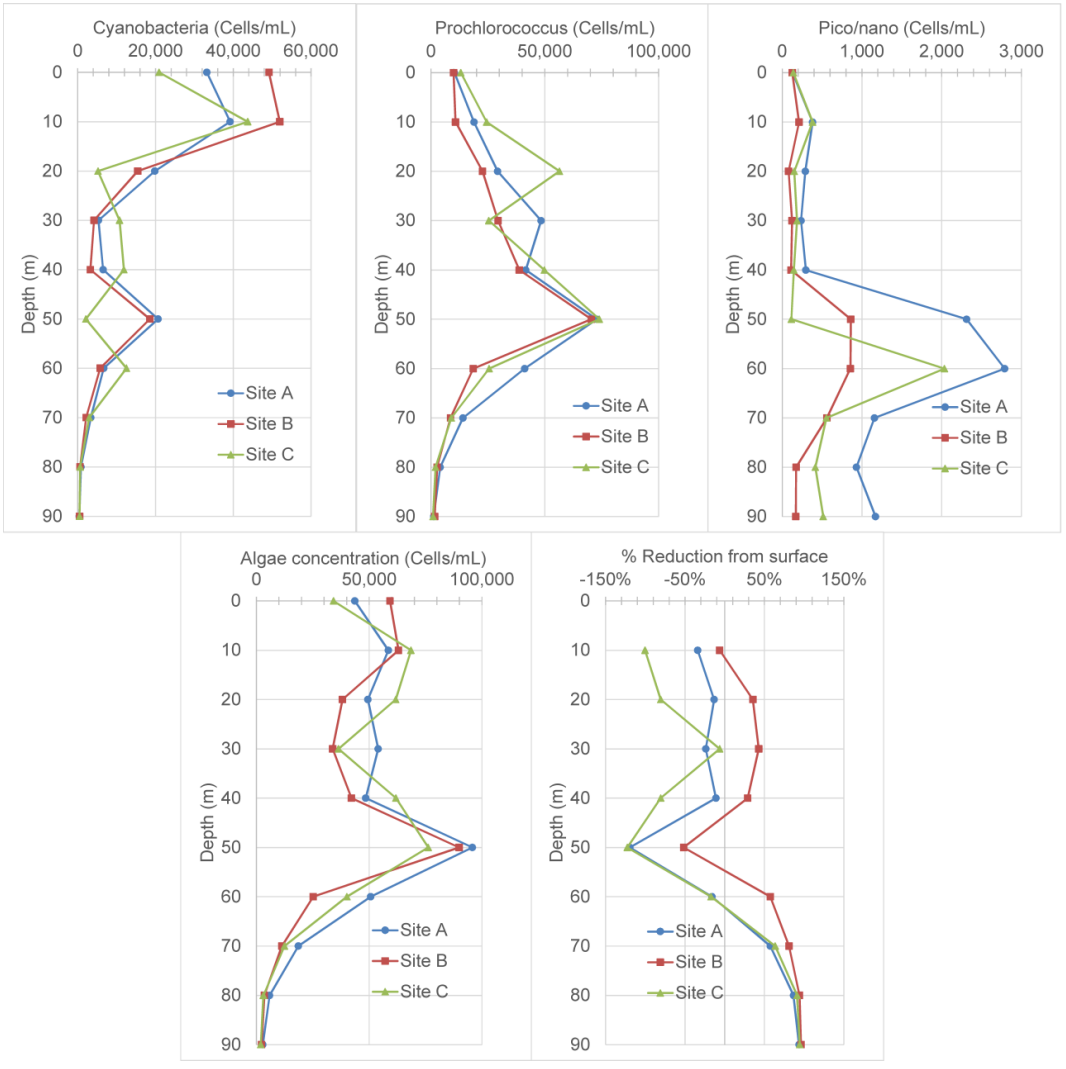

663

664 Fig. 5. Algal composition and concentration data from the three 90 m profiles

Biogeosciences Discuss., https://doi.org/10.5194/bg-2019-59
Manuscript under review for journal Biogeosciences
Discussion started: 13 March 2019

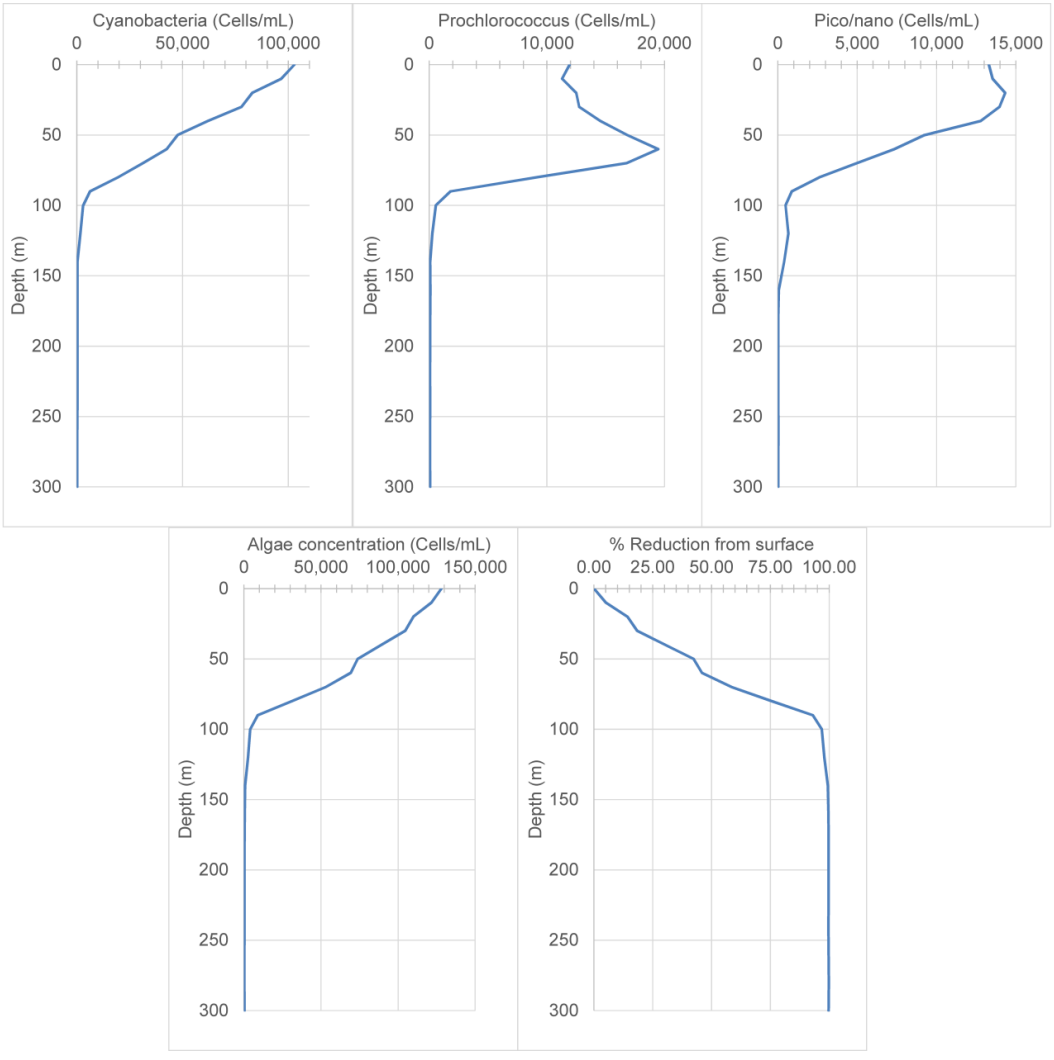

665

666 Fig. 6. Algal composition and concentration data from the 300 m profile

Biogeosciences Discuss., https://doi.org/10.5194/bg-2019-59
Manuscript under review for journal Biogeosciences
Discussion started: 13 March 2019

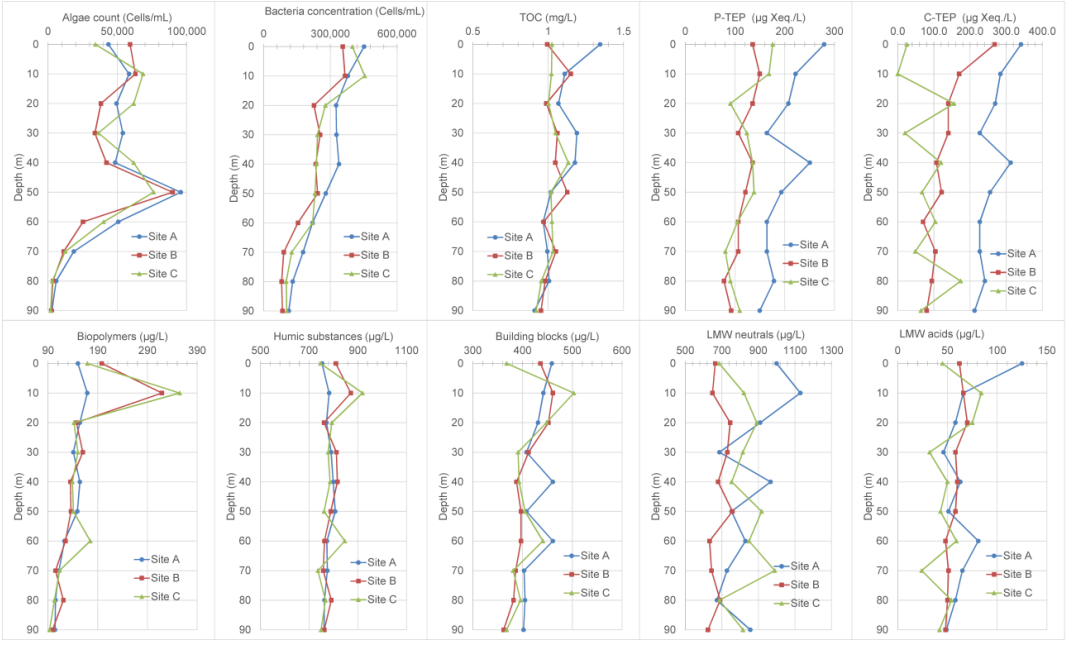

667

668 Fig. 7. Organic carbon concentrations for the three 90 m profiles

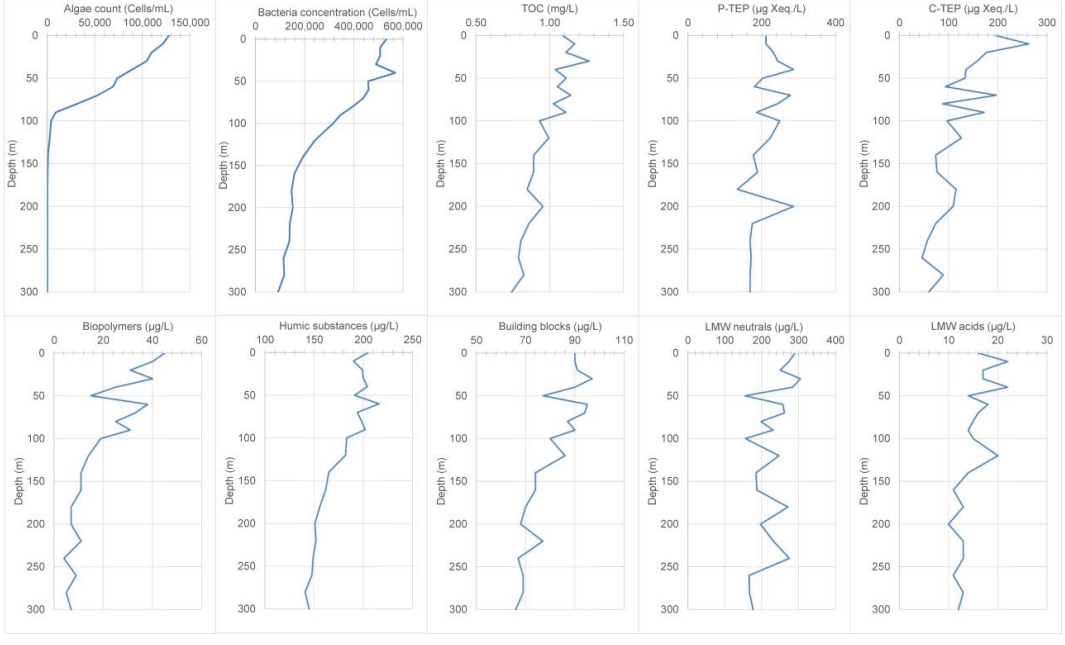

669

670 Fig. 8. Organic carbon concentrations from the 300 m profile